

FreeGAD: A Training-Free yet Effective Approach for Graph Anomaly Detection

Yunfeng Zhao*
Guangxi University
Nanning, China
yunf.zhao@st.gxu.edu.cn

Yixin Liu*
Griffith University
Gold Coast, Australia
yixin.liu@griffith.edu.au

Shiyuan Li*
Guangxi University
Nanning, China
li.shiy511@gmail.com

Qingfeng Chen†
Guangxi University
Nanning, China
qingfeng@gxu.edu.cn

Yu Zheng
Griffith University
Gold Coast, Australia
zhengyu511@gmail.com

Shirui Pan
Griffith University
Gold Coast, Australia
s.pan@griffith.edu.au

Abstract

Graph Anomaly Detection (GAD) aims to identify nodes that deviate from the majority within a graph, playing a crucial role in applications such as social networks and e-commerce. Despite the current advancements in deep learning-based GAD, existing approaches often suffer from high deployment costs and poor scalability due to their complex and resource-intensive training processes. Surprisingly, our empirical findings suggest that the training phase of deep GAD methods, commonly perceived as crucial, may actually contribute less to anomaly detection performance than expected. Inspired by this, we propose **FreeGAD**, a novel training-free yet effective GAD method. Specifically, it leverages an affinity-gated residual encoder to generate anomaly-aware representations. Meanwhile, FreeGAD identifies anchor nodes as pseudo-normal and anomalous guides, followed by calculating anomaly scores through anchor-guided statistical deviations. Extensive experiments demonstrate that FreeGAD achieves superior anomaly detection performance, efficiency, and scalability on multiple benchmark datasets from diverse domains, without any training or iterative optimization.

CCS Concepts

• **Computing methodologies** → **Neural networks**; • **Mathematics of computing** → **Graph algorithms**.

Keywords

Unsupervised Learning, Graph neural networks, Anomaly detection

ACM Reference Format:

Yunfeng Zhao, Yixin Liu, Shiyuan Li, Qingfeng Chen, Yu Zheng, and Shirui Pan. 2025. FreeGAD: A Training-Free yet Effective Approach for Graph Anomaly Detection. In *Proceedings of the 34th ACM International Conference*

*All authors contributed equally to this research.

†Corresponding author.

Permission to make digital or hard copies of all or part of this work for personal or classroom use is granted without fee provided that copies are not made or distributed for profit or commercial advantage and that copies bear this notice and the full citation on the first page. Copyrights for components of this work owned by others than the author(s) must be honored. Abstracting with credit is permitted. To copy otherwise, or republish, to post on servers or to redistribute to lists, requires prior specific permission and/or a fee. Request permissions from permissions@acm.org.

CIKM '25, Seoul, Republic of Korea

© 2025 Copyright held by the owner/author(s). Publication rights licensed to ACM.

ACM ISBN 979-8-4007-2040-6/2025/11

<https://doi.org/10.1145/3746252.3761125>

on Information and Knowledge Management (CIKM '25), November 10–14, 2025, Seoul, Republic of Korea. ACM, New York, NY, USA, 11 pages. <https://doi.org/10.1145/3746252.3761125>

1 Introduction

Graph anomaly detection (GAD) is a critical research area focused on identifying abnormal nodes that significantly deviate from normal patterns within a graph [27, 37]. GAD has been applied to numerous real-world scenarios, such as fraud detection in financial networks, intrusion detection in cybersecurity, and identifying irregularities in social or communication networks [13, 35, 51]. The growing importance of GAD in real-world applications has led to increasing research attention being devoted to developing effective and robust methods for detecting anomalies in graph-structured data [7, 25, 36].

Due to the difficulty of obtaining labeled anomaly data in real-world scenarios, the mainstream GAD methods primarily focus on unsupervised scenarios [2, 8, 36, 37]. While the early shallow GAD methods often face limitations in handling complex and high-dimensional real-world graph data [7], deep learning-based GAD methods have emerged in recent years as the de facto solution, demonstrating superior performance in benchmark datasets [2, 36]. These deep GAD methods leverage graph neural networks (GNNs) as their backbone models and employ anomaly-aware unsupervised techniques or customized objectives for model optimization. After sufficient training, the model output can be transformed into abnormality measurements through specific rules or algorithms. For example, DOMINANT [7] and AnomalyDAE [8] employ graph autoencoder models to reconstruct graph data, using reconstruction errors as indicators of anomalies. CoLA [25] and ANEMONE [14] introduce GNN-based contrastive learning frameworks for GAD, where the degree of mutual agreement between contrastive elements can measure the node abnormality. More recent methods adopt diverse unsupervised learning and anomaly scoring strategies, such as hop counting [11] and local affinity estimation [36], to further raise the bar of GAD performance.

Despite their effectiveness, the costs associated with training these deep GAD models are non-negligible. To achieve optimal detection performance, hundreds of epochs of training are often necessary, leading to high computational costs and prolonged deployment times. As shown in Fig. 1(a), the training time constitutes a substantial portion of the deployment duration for most approaches,

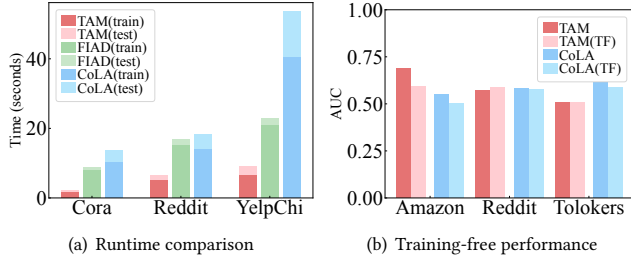


Figure 1: (a): The efficiency of different GAD methods, with the runtime square-rooted for comparison. (b): The difference of GAD methods with and without training.

causing delays in applying anomaly detection to time-sensitive systems and diminishing their practical utility. Moreover, since GNNs require complete graph structures for propagation operations, the training of GNN models typically involves performing backpropagation over the entire graph [6]. As a result, training GNN-based GAD models on large-scale datasets becomes highly challenging due to increased memory requirements, further limiting their scalability and practical applicability in real-world scenarios. As evidence, our experiments in Table 2 show that most GAD methods fail to run on T-Finance dataset (with 39k nodes) on a GPU with 24GB memory. The aforementioned limitations prompt us to consider a question: *Is it truly necessary to heavily train GNN-based GAD models to achieve effective anomaly detection?*

Recalling the framework architectures of mainstream deep GAD approaches, the learnable components mainly lie in the transformation operations within the GNN model, where features are transformed through learnable projections to refine node representations. Apart from this, other components, such as propagation and anomaly scoring, are typically parameter-free, and thus do not require training for optimization. To verify the contribution of model training to the final anomaly detection performance, we modify two representative GAD methods (i.e., CoLA [25] and TAM [36]) into training-free (TF) variants by removing the learnable components. We evaluate their performance against the original models and the comparison is demonstrated in Fig. 1(b). Surprisingly, the training-free variants perform competitively against their fully trained counterparts, with only a 5.0% drop in average. Our observation suggests that model training may not be as critical to anomaly detection performance as previously thought. In this case, a natural question arises: *Can we design a GAD approach that achieves competitive anomaly detection performance without the need for training?*

Motivated by the above question, this paper proposes a training-free yet effective approach for Graph Anomaly Detection, abbreviated as **FreeGAD**. FreeGAD can effectively detect abnormal nodes without the need for training, leveraging a propagation-only encoder to generate node representations and an anchor-based distance measurement module to predict node abnormality. To be more specific, FreeGAD begins with an affinity-gated residual encoder to generate anomaly-aware representations, explicitly capturing the inherent affinity between nodes and their multi-hop

neighbors. After that, an anchor node selection module identifies anchor nodes, which are the most representative samples, serving as pseudo normal and anomaly nodes for guiding the model in discriminating between normal and anomalous patterns. Finally, an anchor-guided anomaly scoring module calculates the abnormality score for each node by measuring its statistical deviation from the anchor nodes, enabling precise identification of anomalies. The entire process operates directly on the data in a single run, without requiring any training or optimization. To verify the effectiveness of FreeGAD, we conduct extensive experiments on 10 real-world benchmark datasets, comparing its performance against state-of-the-art GAD methods. The empirical study demonstrates the advantages of FreeGAD:

- **Superior Detection Performance.** Without the need for training, FreeGAD achieves state-of-the-art performance on 6 out of 10 datasets and competitive performance on the remaining ones. Notably, FreeGAD excels in detecting real anomalies compared to the synthetic ones, which highlights its potential in real-world fraud and intrusion detection scenarios.
- **Extremely Low Time Cost.** Due to its training-free nature, FreeGAD has significantly shorter deployment time compared to baselines, indicating its applicability for time-sensitive applications.
- **Excellent Scalability.** FreeGAD demonstrates enhanced scalability, as it can be effectively applied to large-scale datasets, such as Elliptic with 200k+ nodes, as well as to the over-dense dataset T-Finance with 21m+ edges, highlighting its capacity to handle complex and large-scale graph data.

2 Related Work

2.1 Graph Anomaly Detection

Graph anomaly detection (GAD) aims to identify the nodes that exhibit anomalous behavior or deviate significantly from the normal patterns in a graph.

Earlier studies primarily focus on using shallow learning approaches for GAD [1, 17]. For example, AMEN [33] leveraged the information of ego-network for each node to detect anomalous neighborhoods within attributed networks. ANOMALOUS [32] employs a joint framework with CUR decomposition and residual analysis for GAD. Although these methods do not leverage deep learning techniques, most of them still require iterative optimization for training.

Recent research highlights the effectiveness of deep learning in GAD, utilizing graph neural networks (GNNs) to build powerful GAD models [37, 53]. For instance, DOMINANT [7] employs a graph-convolutional autoencoder (GAE) to reconstruct both the adjacency and attribute matrices, where node anomalies are assessed based on reconstruction errors. SpecAE [20] and AnomalyDAE [8] use advanced GAE architectures to boost the performance of DOMINANT. Apart from reconstruction models, another line of studies, such as CoLA [25] and ANEMONE [14], utilizes contrastive GNN frameworks to learn robust scoring models for anomaly detection. PREM [31] further refines contrastive GAD models by simplifying their architecture and eliminating redundant components. Recently,

Qiao et al. [36] indicate the key role of *local affinity* in detecting anomalous nodes and propose a truncated affinity maximization (TAM) model for GAD. HUGE [30] proposes HALO, a label-free heterogeneity measure estimated from node attributes, for unsupervised node anomaly detection. For all deep learning GAD methods, gradient descent-based optimization is required for model training, which can be time-consuming.

While existing deep GAD methods have demonstrated strong performance, they require iterative training or optimization to achieve strong detection performance, leading to increased deployment time and resource demands. To address this problem, the aim of this paper is to propose a learning-free yet effective baseline model for GAD.

2.2 Graph Neural Networks

Graph neural networks (GNNs) are a neural network architecture designed for graph-structured data, employing a message-passing mechanism with two key operations: *propagation* (P), which facilitates information exchange between neighboring nodes, and *transformation* (T), which updates node embeddings through learnable non-linear projections [49]. Due to their powerful capabilities, GNNs have been successfully applied across a wide range of tasks [18, 19, 23, 24, 40]. Different GNN models leverage diverse propagations and aggregation functions. Frequently utilized P functions comprise averaging aggregation [15], attention aggregation [46], and LSTM aggregation [10], while T operations are typically implemented as one or more perceptron layers followed by non-linear activations.

Most GNN-based models [5, 7, 25, 26, 29] adopt the PTPT structure, which is constructed by sequentially stacking multiple "P-T" operations. Although this design is widely used, it often faces issues of increased runtime and reduced efficiency, and is also prone to overfitting during the training process. Moreover, in some decoupled GNN models [52], propagation and transformation operations are not simply alternated but instead repeat one operation several times before switching to the other. For example, in models such as APPNP [9], SGC [48], and AP-GCN [41], the propagation and transformation operations can be nested cyclically in multiple levels to enhance the expressive power of the model. This design approach provides a more flexible architecture for GNNs that can adapt to different task requirements.

Building on decoupled models, in this paper, we design an affinity-gated residual encoder with multi-hop propagation while discarding feature transformation, which ensures the generation of high-quality representations without requiring training.

3 Preliminaries

Notations. A undirected attributed graph can be denoted as $\mathcal{G} = (\mathcal{V}, \mathcal{E}, \mathbf{X})$, where $\mathcal{V} = \{v_1, \dots, v_n\}$ represents the set of nodes, \mathcal{E} is the set of edges, and $|\mathcal{V}| = n$, $|\mathcal{E}| = e$, respectively. The features of nodes can be described by the node feature matrix $\mathbf{X} \in \mathbb{R}^{n \times m}$, where m is the dimension of features and the i -th row \mathbf{x}_i represents the feature vector of the i -th node v_i . The connection between nodes can be represented by an adjacency matrix $\mathbf{A} \in \{0, 1\}^{n \times n}$, where the i, j -th entry $A_{ij} = 1$ means v_i and v_j are connected and vice versa. The symmetric normalization of the adjacency matrix

is denoted by $\hat{\mathbf{A}} = \tilde{\mathbf{D}}^{-\frac{1}{2}} \tilde{\mathbf{A}} \tilde{\mathbf{D}}^{-\frac{1}{2}}$, where $\tilde{\mathbf{A}} = \mathbf{A} + \mathbf{I}$ represents the adjacency matrix of the undirected graph with the addition of the self-loops and $\tilde{\mathbf{D}}$ is the diagonal degree matrix of $\tilde{\mathbf{A}}$.

Problem Formulation. Considering the sparsity of anomaly labels, this paper focuses on unsupervised graph node anomaly detection (GAD) scenarios. In unsupervised GAD scenario, the node set \mathcal{V} can be divided into anomalous node set \mathcal{V}_a and normal node set \mathcal{V}_n , with $\mathcal{V} = \mathcal{V}_a \cup \mathcal{V}_n$, $\mathcal{V}_a \cap \mathcal{V}_n = \emptyset$, and $|\mathcal{V}_a| = N_a \ll |\mathcal{V}_n| = N_n$. The objective of unsupervised GAD is to learn a scoring function (i.e., GAD model) \mathcal{F} to obtain anomaly score for all nodes in \mathcal{G} : $\mathcal{F}(\mathbf{A}, \mathbf{X}) \rightarrow \mathbf{s} \in \mathbb{R}^n$, where \mathbf{s} is the anomaly scores for all nodes, with each entry s_i indicating the abnormal degree of node v_i , i.e., the probability of v_i belonging to \mathcal{V}_a rather than \mathcal{V}_n .

4 Methodology

In this section, we introduce FreeGAD, a training-free and effective method for graph anomaly detection (GAD). As illustrated in Fig. 2, the overall pipeline of FreeGAD consists of three components: ① *Affinity-gated residual encoder* to generate anomaly-sensitive node representations (Sec. 4.1); ② *Anchor node selection* to choose the pseudo normal/abnormal nodes that characterize the underlying data distribution (Sec. 4.2); and ③ *Anchor-guided anomaly scoring* to measure node-level abnormality by statistically evaluating the distance between the representations of each node and the selected anchor nodes (Sec. 4.3). The following subsections offer a comprehensive explanation of each module.

4.1 Affinity-Gated Residual Encoder

In the first step of FreeGAD, we design an encoder to generate representations of nodes. The representations are expected to incorporate the semantic and structural information of each node, providing anomaly-related cues for effective abnormality prediction. The state-of-the-art GAD methods (e.g., CoLA [25] and TAM [36]) usually employ GCN [15] as encoder, which may suffer from two limitations. *Firstly*, stacking many layers can degrade the representation capability of GCN due to over-smoothing [3] and model degradation issues [52]. This limitation hinders GCN from capturing high-order information from long-range nodes, which is crucial for detecting real-world anomalies. *Secondly*, GCN learns representations by simply averaging ego and neighbor information, which may fail to capture anomaly-sensitive knowledge (e.g. affinity [36]).

To generate high-quality and task-specific representations, we design an advanced, training-free encoder. To address the first limitation, we use a multi-hop propagation-based architecture without feature transformation, which prevents model degradation; also, we introduce a residual design to alleviate over-smoothing problem. To address the second one, we explicitly estimate the affinity from the propagated features and use the affinity to gate the residual connection. In this way, the output affinity-aware representations can better indicate the node-level abnormality. The following paragraphs introduce the detailed procedure of each step.

Multi-Hop Propagation. To capture high-order information in a training-free manner, in FreeGAD, we focus exclusively on propagating node feature representations without introducing additional feature transformation operation with learnable parameters.

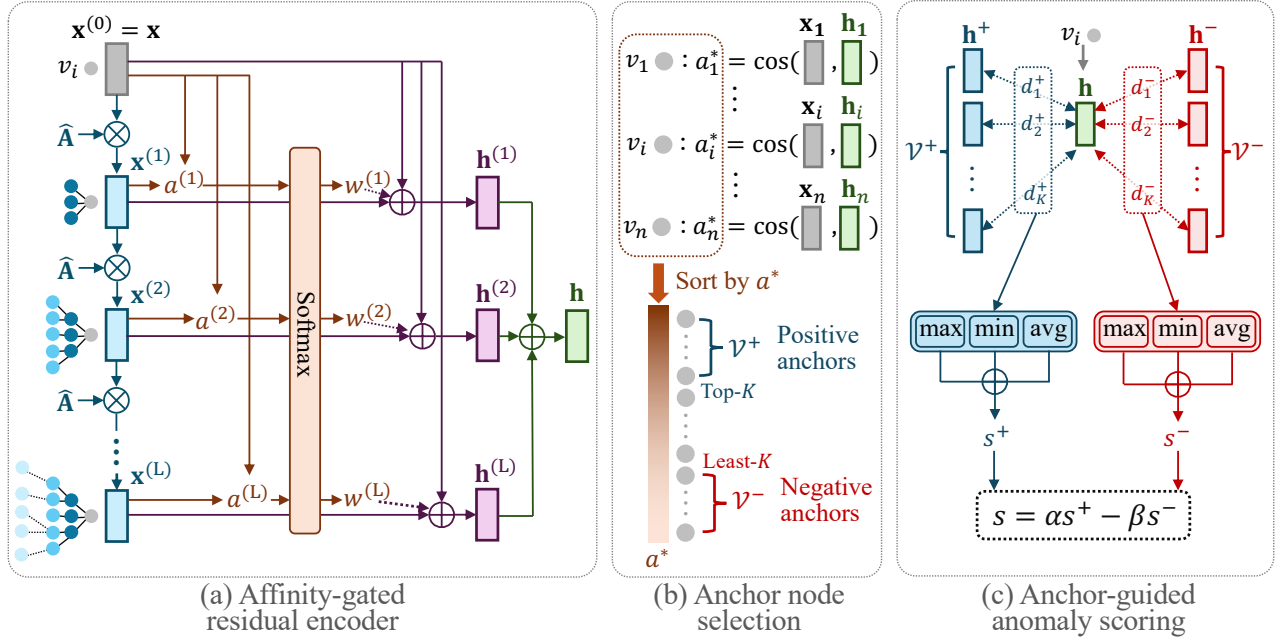


Figure 2: The overall pipeline of FreeGAD. In blocks (a) and (c), we omit the subscript “ i ” for variables x , a , w , h , d , and s for simplicity.

Specifically, we can achieve this by repeatedly performing message propagation operations:

$$\mathbf{X}^{(l)} = \hat{\mathbf{A}}\mathbf{X}^{(l-1)}, \quad (1)$$

where $l \in \{1, \dots, L\}$ is the layer index, L is a pre-defined number of layers, $\mathbf{X}^{(l)}$ is the propagated feature matrix at the l -th layer, and $\hat{\mathbf{A}}$ is the normalized adjacency matrix. The features at the first input layer are denoted as the original features, i.e., $\mathbf{X}^{(0)} = \mathbf{X}$. The propagation-only design not only prevents the model degradation issues caused by excessive transformations [52], but also achieves our training-free design goal by removing the transformations.

Affinity Estimation. As highlighted by Qiao et al. [36], node affinity is a key property that strongly correlates with node abnormality. While they only focus on local affinity between each node and its 1-hop neighbors, in real-world data, the abnormality can also related to high-order affinity, i.e., the similarity between each node and its high-order neighbors [24]. To capture such patterns in the learned representations, in FreeGAD, we estimate multi-order affinity and leverage it during representation generation.

Specifically, we quantify neighborhood-specific affinity by measuring the similarity between the raw features and the propagated features derived from different neighborhoods. For node v_i , the similarity between the l -th propagated feature and the raw feature is calculated as follows:

$$a_i^{(l)} = \frac{\sum_{j=1}^m \mathbf{x}_{ij}^{(0)} \cdot \mathbf{x}_{ij}^{(l)}}{\|\mathbf{x}_i^{(0)}\|^2 \cdot \|\mathbf{x}_i^{(l)}\|^2 + \sigma}, \quad (2)$$

where $\|\cdot\|$ represents the l_2 norm, $\mathbf{x}_{ij}^{(l)}$ stands for the i -th node’s j -th feature, and the σ represents a small value to prevent denominator

tend to 0. After obtaining the feature similarity between a node and its multi-hop neighborhoods, we conduct a layer-wise Softmax-based normalization to obtain the affinity weights:

$$w_i^{(l)} = \frac{\exp(a_i^{(l)})}{\sum_{k=1}^L \exp(a_i^{(k)})}. \quad (3)$$

Affinity-Gated Residual. Once we obtain the normalized affinity at each propagation step, we employ the affinity as a gating scalar for the residual operation between propagated features and original features. Specifically, the representation at the l -th layer, denoting as $\mathbf{h}_i^{(l)}$, can be written as:

$$\mathbf{h}_i^{(l)} = (1 - w_i^{(l)})\mathbf{x}_i^{(l)} + w_i^{(l)}\mathbf{x}_i^{(0)}. \quad (4)$$

According to Eq. (4), the representation of each node can be expressed as the linear combination of its propagated and original features. The gating mechanism ensures that, if a node has a higher affinity with its l -hop neighbors, then its l -layer representation will be closer to the original feature, preserving its original attributes; conversely, if a node exhibits lower affinity with its l -hop neighbors, its l -layer representation will incorporate more information from the propagated features, emphasizing the differences. Such differential treatment not only effectively distinguishes nodes with high and low affinity (which reflects the degree of node abnormality) at the representation level, but also preserves the ego information within the features. Moreover, the residual operation helps mitigate the over-smoothing problem caused by multi-hop propagation, ensuring the informativeness of the representations.

Multi-Hop Mixing. To unify the representations learned at different propagation steps into a single representation, we perform

multi-hop mixing by averaging the representations from each layer:

$$\mathbf{h}_i = \frac{1}{L} \sum_{l=1}^L \mathbf{h}_i^{(l)}, \quad (5)$$

where \mathbf{h}_i is the final representation vector for node v_i . With the mixing operations, the information from different propagation steps is effectively aggregated, enabling the final representation to capture both local and global contextual information.

The representations generated by our affinity-gated residual encoder enjoy several notable merits. **① Multi-scale-aware:** The multi-hop mixing mechanism incorporates information from multi-hop neighbors, which enriches the representation with broader contextual insights. **② Affinity-aware:** Thanks to the affinity-gated residual mechanism, the learned representations effectively capture each node’s affinity with its multi-hop neighbors, thereby reflecting its abnormality accurately. **③ Training-free:** Our encoder has no learnable parameters, eliminating the need for training in the entire learning process. **④ Original space-preserving:** All operations are performed in the original feature space, which facilitates the computation of affinity for anchor node selection in the next subsection.

4.2 Anchor Node Selection

After obtaining the node representations, the next key step is to predict the abnormality (i.e., anomaly score) of each node. However, in unsupervised GAD settings, the inaccessibility of labels complicates the direct supervision of the scoring module. As a result, it is necessary to design a training-free mechanism that can effectively estimate the anomaly scores without relying on labeled data for FreeGAD.

According to the idea of pseudo-label self-supervised learning [42], we design an anchor node-guided anomaly scoring algorithm. Our rationale is to filter out the most representative nodes from the graph as **anchor nodes**, and then measure the degree of abnormality of each node based on its distance to the anchor nodes. To be more specific, we incorporate two types of anchor nodes: **positive anchor nodes** corresponding to the pseudo-normal nodes in the graph, and **negative anchor nodes** corresponding to the nodes that exhibit abnormal characteristics. To select the anchor nodes with a simple criterion, we again rely on the affinity measurement due to its strong correlation with abnormality. Based on the similarity between the representation and raw feature of each node v_i , its affinity a_i^* can be calculated by:

$$a_i^* = \text{sim}(\mathbf{x}_i, \mathbf{h}_i), \quad (6)$$

where $\text{sim}(\cdot)$ represents the similarity function defined according to Eq. (2). By collecting the affinity of all nodes, we can obtain an affinity list, denoted by $\mathbf{a}^* = [a_1^*, a_2^*, \dots, a_n^*]$. Then, we rearrange the list in descending order based on the affinity values, which can be denoted as $\mathbf{a}_{sorted}^* = \text{sort}(\mathbf{a}^*)$. According to the sorted list, we select the top- K nodes with the highest affinity values as the positive anchor nodes:

$$\mathcal{V}^+ = \{v_i \in \mathcal{V} \mid \text{idx}(a_i^*, \mathbf{a}_{sorted}^*) \leq K\}, \quad (7)$$

where $\mathcal{V}^+ = \{v_1^+, v_2^+, \dots, v_K^+\}$ is the set of positive anchor nodes and $\text{idx}(a_i^*, \mathbf{a}_{sorted}^*)$ returns the index of a_i^* within \mathbf{a}_{sorted}^* . In the

same way, the negative anchor nodes can be selected as the top- K nodes with the smallest affinity values:

$$\mathcal{V}^- = \{v_i \in \mathcal{V} \mid \text{idx}(a_i^*, \mathbf{a}_{sorted}^*) \geq n - K + 1\}, \quad (8)$$

where $\mathcal{V}^- = \{v_1^-, v_2^-, \dots, v_K^-\}$ denotes the set of negative anchor nodes. Through the simple selection algorithm, the most representative nodes in a graph can be identified and then serve as a critical clue to predict the abnormality of each node.

4.3 Anchor-Guided Anomaly Scoring

After collecting positive anchor nodes (i.e. pseudo-normal nodes) and negative anchor nodes (i.e. pseudo-abnormal nodes), we utilize an anchor-guided anomaly scoring algorithm to generate the anomaly scores via distance measurement. Our basic assumption is that normal nodes share common patterns with each other and, hence, have closer distances in the representation space; similarly, anomalies may have different shared patterns, leading to their closer representation distances. Therefore, a node that is closer to the positive anchor nodes is potentially more likely to be normal, and vice versa. Motivated by this, we propose to leverage the statistic of the distance measurement between a node v_i and the anchor nodes $\mathcal{V}^+/\mathcal{V}^-$ to estimate the anomaly score of v_i .

Formally, given a node v_i and a positive anchor node v_k^+ , we can calculate the Euclidean distance d_{ik}^+ between their representations, which can be denoted by:

$$d_{ik}^+ = \|\mathbf{h}_i - \mathbf{h}_k^+\|_2. \quad (9)$$

In the same way, we can obtain v_i ’s distance to all positive and negative anchor nodes, denoted as $\mathcal{D}_i^+ = \{d_{i1}^+, \dots, d_{iK}^+\}$ and $\mathcal{D}_i^- = \{d_{i1}^-, \dots, d_{iK}^-\}$, respectively. Considering the diversity of anchor nodes, we combine multiple statistics of the distances \mathcal{D}_i^+ and \mathcal{D}_i^- to obtain a more comprehensive anomaly assessment. Concretely, the positive score s_i^+ for node v_i can be computed by:

$$s_i^+ = \min(\mathcal{D}_i^+) + \max(\mathcal{D}_i^+) + \text{avg}(\mathcal{D}_i^+), \quad (10)$$

where $\min(\cdot)$, $\max(\cdot)$, and $\text{avg}(\cdot)$ extract the minimum, maximum, and average values of the positive distance set \mathcal{D}_i^+ , respectively. In a similar way, the negative score s_i^- can be calculated according to the negative distance set \mathcal{D}_i^- . Finally, we perform a weighted sum of the positive and negative scores to obtain the final anomaly score of the node v_i :

$$s_i = \alpha s_i^+ - \beta s_i^-, \quad (11)$$

where α and β are hyper-parameters between 0 and 1.

It is worth noting that there are no learnable parameters involved in the entire architecture of FreeGAD, which means that the model does not require any training and learning. It also avoids overfitting to specific anomaly patterns caused by training towards specific data. Compared with existing GAD methods such as those based on data reconstruction and the comparative GAD methods that include negative score computation and multiple rounds of estimation [14, 25], FreeGAD also provides higher running efficiency in the anomaly score estimation process.

In general, the overall procedures of FreeGAD are shown in Algo. 1.

Algorithm 1 The Overall Procedure of FreeGAD

Input: Graph \mathcal{G} , Propagation iteration: L , Number of anchor nodes: K , Positive score weight: α , Negative score weight: β .

Output: Anomaly score s .

```

1: Extract feature matrix  $\mathbf{X}$ , adjacency matrix  $\mathbf{A}$  from  $\mathcal{G}$ .
2: // Affinity-gated residual encoder.
3: for  $l = 1:L$  do
4:    $\mathbf{X}^{(l)} \leftarrow \text{Propagation}(\mathbf{X}, \mathbf{A}; L)$  via Eq. (1)
5: end for
6: for  $\mathbf{x}_i \in \mathbf{X}$  do
7:   for  $l = 1:L$  do
8:      $\mathbf{a}_i^{(l)} \leftarrow \text{Similarity}(\mathbf{x}_i^{(0)}, \mathbf{x}_i^{(l)})$  via Eq. (2)
9:   end for
10:  Calculate  $\mathbf{W}_i = \{w_i^{(1)}, \dots, w_i^{(L)}\} \leftarrow \text{Softmax}(\mathbf{a}_i)$  via Eq. (3)
11:  for  $l = 1:L$  do
12:     $\mathbf{h}_i^{(l)} \leftarrow \text{Gating mechanism}$  via Eq. (4)
13:  end for
14:   $\mathbf{h}_i \leftarrow \text{Mean}(\mathbf{h}_i^{(1)}, \dots, \mathbf{h}_i^{(L)})$  via Eq. (5)
15: end for
16: // Anchor node selection.
17: Calculate the affinity  $\mathbf{a}^* = [a_1^*, a_2^*, \dots, a_n^*]$  of raw feature
     $[\mathbf{x}_1, \mathbf{x}_2, \dots, \mathbf{x}_n]$  and representation  $[\mathbf{h}_1, \mathbf{h}_2, \dots, \mathbf{h}_n]$  via Eq. (6)
18: The set of positive anchor nodes  $\mathcal{V}^+ = \{v_1^+, v_2^+, \dots, v_K^+\} \leftarrow$ 
     $\text{Top}(\mathbf{a}^*, K, \mathbf{h})$  via Eq. (7)
19: The set of negative anchor nodes  $\mathcal{V}^- = \{v_1^-, v_2^-, \dots, v_K^-\} \leftarrow$ 
     $\text{Bottom}(\mathbf{a}^*, K, \mathbf{h})$  via Eq. (8)
20: // Anchor-guided anomaly scoring.
21: for  $\mathbf{h}_i \in \mathbf{h}$  do
22:    $\mathcal{D}_i^+ = \{d_{i1}^+, \dots, d_{iK}^+\}$  as the distances between the target node
       $\mathbf{h}_i$  and each of the  $K$  positive anchor nodes.
23:    $\mathcal{D}_i^- = \{d_{i1}^-, \dots, d_{iK}^-\}$  as the distances between the target node
       $\mathbf{h}_i$  and each of the  $K$  negative anchor nodes.
24:   Calculate the predicted scores  $(s_i^+, s_i^-)$  of anchor node via
      Eq. (10)
25:   Calculate the anomaly score  $s_i$  via Eq. (11)
26: end for

```

4.4 Complexity Analysis

The time complexity of FreeGAD primarily consists of three main components: ① **Affinity-gated residual encoder.** The overall time complexity for this component is $O(emL + nL + 3nmL)$, where e , n , and m represent the number of edges, nodes and the dimension of the feature, respectively, and L is the number of propagation layers. The term emL accounts for the feature propagation process, while the term nmL is the complexity associated with feature similarity calculation, weighted summation, and the average of different propagation layers. ② **Anchor node selection.** The time complexity for the selection of anchor nodes is $O(nm + 2nK)$, where K denotes the number of selected anchor nodes (positive and negative). The first term nm , corresponds to the calculation of the similarity between the node representation and its raw feature, while the second part, $2nK$, represents the process of selecting the anchor nodes. ③ **Anchor-guided anomaly scoring.** Finally, the time complexity to calculate the anomaly score using the anchor-guided approach

Table 1: Statistics of the datasets.

Name	#Nodes	#Edges	#Dim.	%Ano.
Dataset with real anomalies				
Amazon	10,244	175,608	25	6.76
Reddit	10,984	168,016	64	3.33
Tolokers	11,758	519,000	10	21.8
YelpChi	23,831	49,315	32	5.10
T-Finance	39,357	21,222,543	10	4.60
Questions	48,921	153,540	301	2.98
Elliptic	203,769	234,355	166	2.23
Datasets with injected anomalies				
Cora	2,708	5,429	1,433	5.53
BlogCatalog	5,196	171,743	8,189	5.77
Flickr	7,575	239,738	12,047	5.94

is $O(nmK)$. Therefore, the overall time complexity of FreeGAD is $O(m(eL + 3nL + n + nK) + nL + 2nK)$.

5 Experiments

5.1 Experimental Setup

Datasets. To validate the performance of our proposed method, we carried out comparative experiments on 10 benchmark datasets [25, 43] across multiple domains, including 2 co-review networks (Amazon and YelpChi [28, 38]), 4 social networks (Reddit, Questions, BlogCatalog, and Flickr [7, 16, 34, 45]), a work collaboration network (Tolokers [34]), a transaction network (T-Finance [44]), a payment flow network (Elliptic [47]), and a citation network (Cora [39]). Seven of them are datasets containing real-world anomalies, while the remaining three have artificially injected anomalies [7]. The specific details of these datasets are outlined in Table 1.

Baselines. We compare FreeGAD with both shallow methods and state-of-the-art (SOTA) deep methods for unsupervised graph anomaly detection (GAD). Specifically, we include 2 shallow GAD methods, i.e., Radar [17] and ANOMALOUS [32], as well as 8 deep GAD methods, i.e., DOMINANT [7], AnomalyDAE [8], CoLA [25], CONAD [50], PREM [31], TAM [36], GADAM [4], and FIAD [2]. Among them, the 2 shallow GAD methods are based on the PyGOD implementation [21, 22], where all baselines hyperparameters are set based on the paper, and datasets not contained in the paper perform grid-specific random searches.

Metrics. Following the existing benchmark [43], we consider two metrics for evaluation: Area Under the Receiver Operating Characteristic Curve (AUROC) and Area Under the Prevision Recall Curve (AUPRC). We report the average AUROC/AUPRC across 5 trials.

Implementation Details. For hyper-parameter settings, we perform a specific set of random searches to select the key hyperparameters in FreeGAD: α, β : floats between 0 and 1, L : integers between 1 and 20, and K : integers between 10 and 100. The experiments were conducted using Python 3.8.19, CUDA 12.1, PyTorch 2.1.2, and DGL 1.1.3 on a Linux server with an Intel i5-13600K CPU and an NVIDIA RTX 3090 GPU (24GB). Our code is available at <https://github.com/yunf-zhao/FreeGAD>.

Table 2: Anomaly detection performance in terms of AUROC and AUPRC (in percent, mean \pm std). The best results are highlighted in bold and underlined. OOM: out-of-memory (24GB GPU). OOT: out-of-time (12 hours). We do not report the standard deviation of FreeGAD since it is a training-free method, and its results are deterministic, without any randomness introduced by training processes or initialization.

Metric	Method	Amazon	Reddit	Tolokers	YelpChi	T-Finance	Questions	Elliptic	Cora	BlogCatalog	Flickr
AUROC	Radar	55.43 \pm 0.00	51.22 \pm 0.00	51.71 \pm 0.00	50.61 \pm 0.00	OOM	OOM	OOM	69.32 \pm 0.00	61.16 \pm 0.00	59.52 \pm 0.00
	ANOMALOUS	55.46 \pm 0.00	55.95 \pm 4.78	46.48 \pm 0.28	48.77 \pm 1.04	OOM	OOM	OOM	69.38 \pm 0.00	70.86 \pm 0.01	59.52 \pm 0.00
	DOMINANT	49.56 \pm 0.65	55.70 \pm 0.77	54.43 \pm 0.11	41.87 \pm 1.87	OOM	OOM	OOM	88.92 \pm 0.14	76.34 \pm 0.29	77.19 \pm 1.59
	AnomalyDAE	51.60 \pm 3.31	55.18 \pm 0.43	52.20 \pm 2.94	59.45 \pm 2.32	OOT	OOT	OOT	80.66 \pm 0.25	75.61 \pm 0.02	74.87 \pm 0.09
	CoLA	55.23 \pm 0.94	58.24 \pm 0.44	61.17 \pm 0.37	36.46 \pm 0.58	23.45 \pm 0.19	46.37 \pm 0.37	OOM	89.59 \pm 0.31	78.30 \pm 0.21	70.37 \pm 0.39
	CONAD	51.02 \pm 0.23	54.11 \pm 0.59	49.47 \pm 2.36	56.65 \pm 1.07	OOM	OOM	OOM	71.82 \pm 0.02	72.54 \pm 0.02	72.82 \pm 0.02
	TAM	68.87 \pm 0.72	57.17 \pm 0.13	50.88 \pm 0.00	OOM	OOM	OOM	OOM	92.35 \pm 0.23	75.58 \pm 0.20	73.26 \pm 0.45
	PREM	62.61 \pm 11.85	51.87 \pm 6.15	53.48 \pm 4.04	73.93 \pm 1.51	75.30 \pm 12.31	57.16 \pm 1.29	71.23 \pm 11.08	95.11 \pm 0.23	75.06 \pm 0.74	86.53 \pm 0.37
	GADAM	67.09 \pm 3.12	58.18 \pm 0.38	55.42 \pm 0.56	65.53 \pm 1.66	80.20 \pm 7.85	43.70 \pm 0.37	56.42 \pm 0.35	93.93 \pm 0.25	81.58 \pm 0.18	72.26 \pm 0.21
	FIAD	52.36 \pm 8.07	55.72 \pm 1.03	49.73 \pm 1.98	43.27 \pm 3.19	OOM	OOM	OOM	87.43 \pm 1.31	75.47 \pm 2.02	77.01 \pm 2.01
	FreeGAD	88.57	57.21	67.35	78.55	92.13	64.27	77.25	84.85	74.84	74.73
	Radar	7.30 \pm 0.00	3.53 \pm 0.00	23.24 \pm 0.00	5.88 \pm 0.00	OOM	OOM	OOM	11.86 \pm 0.00	14.80 \pm 0.00	19.88 \pm 0.00
	ANOMALOUS	7.30 \pm 0.00	3.86 \pm 0.56	20.14 \pm 0.00	5.51 \pm 0.15	OOM	OOM	OOM	25.23 \pm 0.00	30.62 \pm 0.00	19.88 \pm 0.00
AUPRC	DOMINANT	6.08 \pm 0.08	3.71 \pm 0.06	27.95 \pm 0.03	4.24 \pm 0.34	OOM	OOM	OOM	37.81 \pm 0.44	34.55 \pm 0.05	37.10 \pm 0.05
	AnomalyDAE	7.30 \pm 1.18	3.71 \pm 0.02	26.82 \pm 1.12	7.53 \pm 0.59	OOT	OOT	OOT	26.71 \pm 0.61	23.01 \pm 0.09	16.78 \pm 0.24
	CoLA	8.28 \pm 0.43	4.01 \pm 0.05	27.25 \pm 0.31	3.75 \pm 0.06	2.79 \pm 0.05	2.55 \pm 0.02	OOM	45.79 \pm 2.66	27.09 \pm 0.98	21.36 \pm 0.31
	TAM	29.73 \pm 1.28	4.32 \pm 0.03	22.98 \pm 0.00	OOM	OOM	OOM	OOM	48.24 \pm 1.54	33.88 \pm 0.77	24.70 \pm 1.87
	PREM	8.96 \pm 2.38	3.95 \pm 0.73	23.25 \pm 1.67	10.67 \pm 1.34	33.05 \pm 24.39	3.49 \pm 0.24	7.33 \pm 3.38	65.99 \pm 0.23	37.31 \pm 0.74	46.37 \pm 0.37
	GADAM	15.87 \pm 7.48	5.01 \pm 0.23	23.65 \pm 0.35	10.14 \pm 0.32	15.72 \pm 6.12	2.52 \pm 0.10	3.03 \pm 0.05	71.83 \pm 1.91	37.36 \pm 0.36	23.19 \pm 0.43
	CONAD	6.23 \pm 0.03	4.31 \pm 0.10	21.13 \pm 0.11	7.19 \pm 0.44	OOM	OOM	OOM	24.86 \pm 0.05	33.01 \pm 0.00	37.57 \pm 0.01
	FIAD	6.71 \pm 1.23	3.74 \pm 0.04	29.31 \pm 0.82	4.32 \pm 0.35	OOM	OOM	OOM	29.31 \pm 3.69	25.44 \pm 6.53	19.55 \pm 3.56
	FreeGAD	75.06	3.85	32.17	15.80	73.71	7.01	6.51	49.75	34.03	38.68

Table 3: Training and testing time of baselines and FreeGAD in seconds. The shortest overall times are highlighted in bold and underlined.

Method	Amazon		Reddit		Tolokers		YelpChi		Cora		BlogCatalog		Flickr	
	train	test	train	test	train	test	train	test	train	test	train	test	train	test
Radar	2.0061	0.0204	1.8485	0.0213	1.9994	0.0229	5.8551	0.0865	0.4789	0.008	1.4281	0.1333	1.8316	0.4085
ANOMALOUS	2.1543	0.0135	2.3067	0.0101	2.2285	0.0092	7.0728	0.027	1.252	0.0102	23	0.1734	70	0.5362
DOMINANT	2.3293	0.1633	2.6146	0.1886	2.8165	0.2138	11	0.8201	0.5937	0.0409	4.5385	0.4315	12	1.2824
AnomalyDAE	113	1.1018	118	1.2149	134	1.4219	345	3.4737	32	0.3022	101	0.923	139	1.3636
CoLA	247	20	196	18	172	15	1642	167	111	10	161	15	236	22
CONAD	12	1.3023	13	1.3489	13	1.561	39	4.4816	1.85	0.586	14	1.0551	20	1.7071
TAM	46	1.2557	27	1.4499	73	1.5347	44	5.4196	3.0339	0.2301	42	0.4958	59	0.8114
PREM	0.4613	0.0066	0.3637	0.0075	0.3471	0.0065	0.508	0.0108	0.3056	0.0042	0.9174	0.0054	1.8403	0.0075
GADAM	1.0099	0.0102	0.8122	0.0098	0.8889	0.0124	0.738	0.0213	0.7409	0.0054	1.6262	0.007	2.199	0.0085
FIAD	227	2.0116	233	2.1419	242	2.1964	442	3.4145	67	0.497	215	1.9857	257	2.0871
FreeGAD	0.0317		0.0338		0.0141		0.0357		0.0601		0.1641		0.3142	

5.2 Performance Comparison

The comparison results on seven real-world graph datasets and three injected anomaly datasets (Cora, BlogCatalog, Flickr) are reported in Table 2. From these results, we have the following observations. ❶ FreeGAD demonstrates superior performance compared to SOTA approaches across seven real-world datasets, achieving better results on both evaluation metrics in most cases, with the sole exceptions being AUPRC on Elliptic and both AUROC and AUPRC on Reddit. These results demonstrate the strong effectiveness of

our training-free method across various benchmarks. ❷ While FreeGAD does not achieve SOTA performance on the three injected anomaly datasets, it consistently outperforms traditional non-deep-learning models (e.g., Radar and ANOMALOUS) and maintains competitive performance with leading deep-learning approaches such as Dominant. Additionally, it’s important to note that the community has recently deemed injection-based datasets as unreasonable [12]. Existing methods might achieve better performance with specific designs, suggesting that future evaluations will likely

Table 4: Maximum GPU memory usage (in MB) during training and testing for baselines and FreeGAD

Method	Amazon		Reddit		Tolokers		YelpChi		Cora		BlogCatalog		Flickr	
	train	test	train	test	train	test	train	test	train	test	train	test	train	test
Radar	2814	2416	3257	2796	3715	3187	15202	13036	316	288	2248	1770	4797	3766
ANOMALOUS	1223	1223	1426	1426	1605	1605	6548	6548	263	263	2426	2111	5185	4502
DOMINANT	2850	2035	3290	2351	3759	2682	15284	10910	272	228	1448	1225	3046	2567
AnomalyDAE	3364	3335	3865	3844	4441	4403	17978	17945	343	338	1879	1847	3949	3903
CoLA	423	404	487	467	552	532	2193	2173	79	63	432	376	922	729
CONAD	2452	1639	2815	1876	3246	2173	13076	8706	253	167	1677	1185	3538	2488
TAM	3968	3842	4536	4351	5150	4899	19742	17590	440	551	1535	1620	3036	3056
PREM	91	34	109	43	114	49	219	84	111	59	1191	555	2510	1149
GADAM	96	35	98	33	109	40	153	38	108	51	746	371	1515	756
FIAD	4085	3281	4710	3784	5413	4351	21817	17471	450	364	2605	2073	5498	4361
FreeGAD	32		30		74		30		112		1144		2445	

focus on real anomalous datasets. ③ Due to its training-free nature, FreeGAD is not affected by random initialization or stochastic training processes, leading to its consistent and stable performance on all datasets. In contrast, training-based methods often suffer from performance fluctuations caused by randomness in training processes, such as weight initialization. ④ FreeGAD demonstrates strong scalability, achieving state-of-the-art results on large-scale datasets like T-Finance and Elliptic, where many baseline methods encounter out-of-memory (OOM) issues. This confirms FreeGAD’s suitability for handling graphs with extensive data.

5.3 Efficiency Analysis

To investigate the running efficiency of FreeGAD, we compare the whole runtime of FreeGAD with the training and testing time of baseline methods, and the results are illustrated in Table 3. It is observed that FreeGAD eliminates the need for a training phase, which drastically reduces its overall computation cost. In contrast, training-based methods require significant time for model optimization, with some methods (e.g., CoLA and AnomalyDAE) taking hundreds of seconds on certain datasets, limiting their applicability. Moreover, FreeGAD achieves testing times comparable to, or even better than, many baseline methods. For instance, on BlogCatalog and Flickr datasets, its testing time is substantially lower than methods such as TAM and FIAD, highlighting its efficiency.

In addition, we compare the peak memory usage during training and testing between FreeGAD and various baselines, as shown in Table 4. Notably, FreeGAD demonstrates significantly lower memory consumption on 4 out of 7 benchmark datasets. While CoLA, PREM, and GADAM come closest to FreeGAD, they still consume several times more memory on average, and other baselines often use tens to hundreds of times more. On the remaining three datasets (Cora, BlogCatalog, and Flickr), FreeGAD does not achieve the lowest memory usage, perhaps due to their high feature dimensionality (over 1,000 dimensions per node as shown in Table 1). Unlike methods that apply feature transformation or dimensionality reduction, FreeGAD operates directly on the raw high-dimensional data, resulting in higher memory consumption. Nonetheless, even on these

Table 5: Performance of FreeGAD and its variants in terms of AUROC (in percent). The best results are highlighted in bold and underlined.

Variant	Cora	Reddit	YelpChi	Elliptic
FreeGAD	<u>84.85</u>	<u>57.21</u>	<u>78.55</u>	<u>77.25</u>
w/o Multi-hop	66.80	48.62	54.85	56.21
w/o Anchor	28.62	52.70	75.16	52.13
w/o Negative	30.83	54.05	78.55	52.84
w/o Positive	84.83	48.24	25.58	65.61
w/ Max Score	70.21	54.03	73.85	76.48
w/ Min Score	77.34	56.78	75.34	76.34
w/ Avg Score	84.68	55.99	77.25	41.37

challenging datasets, FreeGAD still outperforms most baselines, including DOMINANT and TAM.

To sum up, FreeGAD achieves significant computational advantages without compromising on performance, highlighting its applications in scenarios where rapid deployment and adaptation are critical.

5.4 Ablation Study

To verify the effectiveness of each key component and design in FreeGAD, we conduct an ablation study by introducing several variants of FreeGAD for comparison.

We compare FreeGAD with four variants that each exclude a key component: ① **w/o Multi-hop**, where the representations at the last layer serve as the final representations; ② **w/o Anchor**, where anchor nodes are randomly selected rather than using affinity-based selection; ③ **w/o Negative** and **w/o Positive**, where only positive or negative score contributes to the final anomaly score. In the upper part of Table 5, we can observe that all key components of FreeGAD contribute significantly to its performance. Removing the multi-hop mechanism (**w/o Multi-hop**) results in a substantial performance drop across all datasets, confirming the

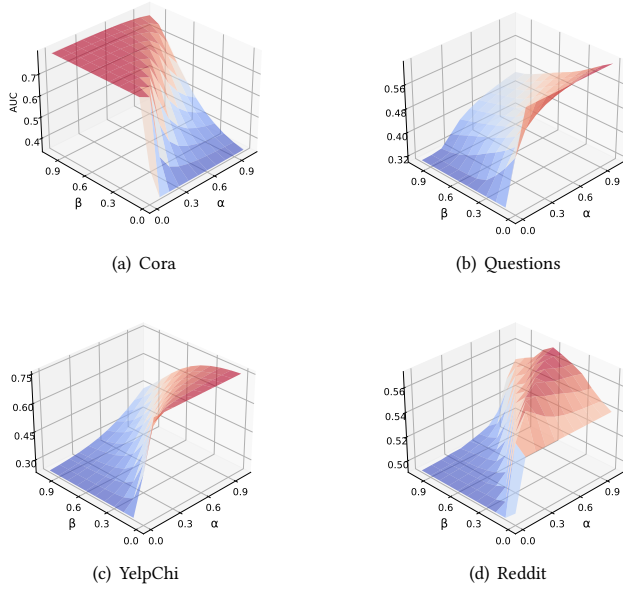


Figure 3: The sensitivity of FreeGAD in terms of α and β .

effectiveness of our affinity-gated residual encoder designed under TAM’s “one-class homophily” principle [36]. Specifically, the encoder leverages this principle to amplify the differences between normal and anomalous nodes, facilitating anomaly pattern detection. The performance degradation in the **w/o Anchor** variant demonstrates that affinity-based anchor selection is crucial for effectively distinguishing anomalies. Furthermore, excluding either positive or negative scoring (**w/o Positive** or **w/o Negative**) leads to noticeable declines, indicating the complementary role of both scores in achieving robust anomaly detection.

Furthermore, we make separated evaluation using only the maximum score (**w/ Max Score**), only the minimum score (**w/ Min Score**), and only the average score (**w/ Avg Score**) to demonstrate the benefit of their combination (lower part of Table 5). On the citation network (Cora), the Avg outperforms both Max and Min, more effectively capturing anomalous behaviors. In social networks (Reddit), Min excels at detecting extreme social anomalies. On the co-review network (YelpChi), Avg again leads by more accurately identifying anomalous reviews. For fraud detection (Elliptic), Max and Min both surpass Avg by pinpointing subtle deviations in financial behavior. Overall, combining all three metrics yields a more comprehensive anomaly score that consistently outperforms any single measure across diverse domains.

5.5 Parameter Analysis

We investigate the impact of key hyper-parameters, i.e., the scoring trade-off weight α and β (in Eq. (11)), the propagation layer L and the anchor nodes number K to the performance of FreeGAD.

Trade-off Weight α and β . The results of sensitivity study for α and β are shown in Fig. 3. According to the results, we can see

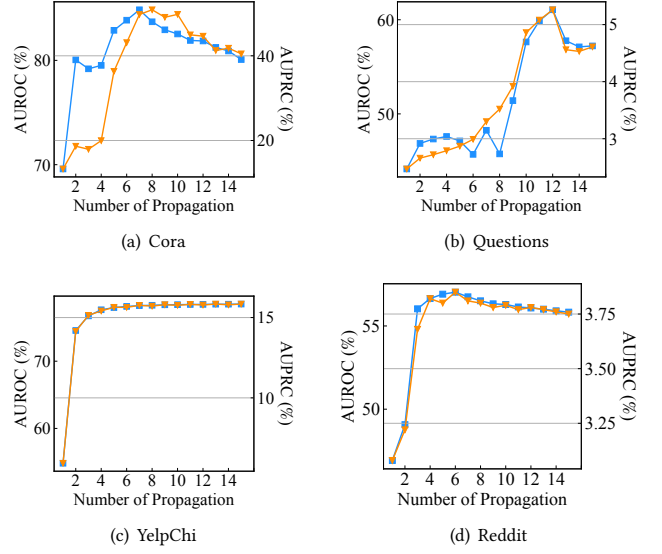


Figure 4: The sensitivity of FreeGAD on layer number L .

that for different datasets, the reliances on α and β are quite different. For example, Cora(citation) requires a higher β , indicating the contribution of negative scores; in contrast, Questions(social), Reddit(social) and YelpChi(co-review) requires a higher α , highlighting the importance of positive scores in anomaly detection. This disparity suggests that the optimal balance between positive and negative contributions varies depending on the dataset’s domain-specific anomaly patterns.

Propagation Layer L . Fig. 4 shows the effect by the propagation layer L , where a larger L (usually $L \geq 8$) is preferred for all four datasets. This indicates that considering multi-hop neighbors is crucial for effective anomaly detection in FreeGAD. Meanwhile, it also indicates that the shallow GNNs in existing GAD methods may lead to suboptimal performance.

6 Conclusion

In this paper, we proposed FreeGAD, a novel training-free method for graph anomaly detection (GAD) that eliminates the need for resource-intensive training processes, addressing the scalability and deployment challenges of traditional approaches. FreeGAD uses an affinity-gated residual encoder to generate anomaly-aware representations and identifies anchor nodes as pseudo-normal and anomalous guides for effective anomaly scoring. Extensive experiments on benchmark datasets demonstrate that FreeGAD achieves superior performance, efficiency, and scalability compared to state-of-the-art methods, which highlights the potential of training-free approaches in advancing GAD research.

Acknowledgments

This work was partially supported by the Specific Research Project of Guangxi for Research Bases and Talents (GuiKe AD24010011), the Key Research & Development Program Project of Guangxi (GuiKe AB25069095).

GenAI Usage Disclosure

Generative AI tools were utilized solely for the purpose of language polishing in this paper. All other components of the research, including but not limited to code, figures, and tables, were developed without the assistance of Generative AI tools.

References

- [1] Leman Akoglu, Hanghang Tong, and Danai Koutra. 2015. Graph based anomaly detection and description: a survey. *Data mining and knowledge discovery* 29, 3 (2015), 626–688.
- [2] Aoge Chen, Jianshe Wu, and Hongtao Zhang. 2025. FIAD: Graph anomaly detection framework based feature injection. *Expert Systems with Applications* 259 (2025), 125216.
- [3] Deli Chen, Yankai Lin, Wei Li, Peng Li, Jie Zhou, and Xu Sun. 2020. Measuring and relieving the over-smoothing problem for graph neural networks from the topological view. In *Proceedings of the AAAI conference on artificial intelligence*, Vol. 34. 3438–3445.
- [4] Jingyan Chen, Guanghui Zhu, Chunfeng Yuan, and Yihua Huang. 2024. Boosting Graph Anomaly Detection with Adaptive Message Passing. In *The Twelfth International Conference on Learning Representations*.
- [5] Qingfeng Chen, Shiyuan Li, Yixin Liu, Shirui Pan, Geoffrey I Webb, and Shichao Zhang. 2025. Uncertainty-Aware Graph Neural Networks: A Multihop Evidence Fusion Approach. *IEEE Transactions on Neural Networks and Learning Systems* (2025).
- [6] Wei-Lin Chiang, Xuanqing Liu, Si Si, Yang Li, Samy Bengio, and Cho-Jui Hsieh. 2019. Cluster-gcn: An efficient algorithm for training deep and large graph convolutional networks. In *Proceedings of the 25th ACM SIGKDD international conference on knowledge discovery & data mining*. 257–266.
- [7] Kaize Ding, Jundong Li, Rohit Bhanushali, and Huan Liu. 2019. Deep anomaly detection on attributed networks. In *Proceedings of the 2019 SIAM international conference on data mining*. SIAM, 594–602.
- [8] Haoyi Fan, Fengbin Zhang, and Zuoyong Li. 2020. Anomalydae: Dual autoencoder for anomaly detection on attributed networks. In *ICASSP 2020–2020 IEEE International Conference on Acoustics, Speech and Signal Processing (ICASSP)*. IEEE, 5685–5689.
- [9] Johannes Gasteiger, Aleksandar Bojchevski, and Stephan Günnemann. 2018. Predict then propagate: Graph neural networks meet personalized pagerank. *arXiv preprint arXiv:1810.05997* (2018).
- [10] Will Hamilton, Zitao Ying, and Jure Leskovec. 2017. Inductive representation learning on large graphs. *Advances in neural information processing systems* 30 (2017).
- [11] Tianjin Huang, Yulong Pei, Vlado Menkovski, and Mykola Pechenizkiy. 2022. Hop-count based self-supervised anomaly detection on attributed networks. In *Joint European conference on machine learning and knowledge discovery in databases*. Springer, 225–241.
- [12] Yihong Huang, Liping Wang, Fan Zhang, and Xuemin Lin. 2023. Unsupervised graph outlier detection: Problem revisit, new insight, and superior method. In *2023 IEEE 39th International Conference on Data Engineering (ICDE)*. IEEE, 2565–2578.
- [13] Riadul Islam, Rafi Ud Daula Refat, Sai Manikanta Yerram, and Hafiz Malik. 2020. Graph-based intrusion detection system for controller area networks. *IEEE Transactions on Intelligent Transportation Systems* 23, 3 (2020), 1727–1736.
- [14] Ming Jin, Yixin Liu, Yu Zheng, Lianhua Chi, Yuan-Fang Li, and Shirui Pan. 2021. Anemone: Graph anomaly detection with multi-scale contrastive learning. In *Proceedings of the 30th ACM international conference on information & knowledge management*. 3122–3126.
- [15] TN Kipf. 2016. Semi-Supervised Classification with Graph Convolutional Networks. *arXiv preprint arXiv:1609.02907* (2016).
- [16] Srikanth Kumar, Xikun Zhang, and Jure Leskovec. 2019. Predicting dynamic embedding trajectory in temporal interaction networks. In *Proceedings of the 25th ACM SIGKDD international conference on knowledge discovery & data mining*. 1269–1278.
- [17] Jundong Li, Harsh Dani, Xia Hu, and Huan Liu. 2017. Radar: Residual analysis for anomaly detection in attributed networks. In *IJCAI*, Vol. 17. 2152–2158.
- [18] Shiyuan Li, Yixin Liu, Qingfeng Chen, Geoffrey I Webb, and Shirui Pan. 2024. Noise-Resilient Unsupervised Graph Representation Learning via Multi-Hop Feature Quality Estimation. In *Proceedings of the 33rd ACM International Conference on Information and Knowledge Management*. 1255–1265.
- [19] Shiyuan Li, Yixin Liu, Qingsong Wen, Chengqi Zhang, and Shirui Pan. 2025. Assemble your crew: Automatic multi-agent communication topology design via autoregressive graph generation. *arXiv preprint arXiv:2507.18224* (2025).
- [20] Yuening Li, Xiao Huang, Jundong Li, Mengnan Du, and Na Zou. 2019. Specac: Spectral autoencoder for anomaly detection in attributed networks. In *Proceedings of the 28th ACM international conference on information and knowledge management*. 2233–2236.
- [21] Kay Liu, Yingdong Dou, Xueying Ding, Xiyang Hu, Ruitong Zhang, Hao Peng, Lichao Sun, and Philip S Yu. 2024. Pygod: A python library for graph outlier detection. *Journal of Machine Learning Research* 25, 141 (2024), 1–9.
- [22] Kay Liu, Yingdong Dou, Yue Zhao, Xueying Ding, Xiyang Hu, Ruitong Zhang, Kaize Ding, Canyu Chen, Hao Peng, Kai Shu, et al. 2022. Bond: Benchmarking unsupervised outlier node detection on static attributed graphs. *Advances in Neural Information Processing Systems* 35 (2022), 27021–27035.
- [23] Yixin Liu, Thalaiyasingam Ajanthan, Hisham Husain, and Vu Nguyen. 2024. Self-supervision improves diffusion models for tabular data imputation. In *Proceedings of the 33rd ACM International Conference on Information and Knowledge Management*. 1513–1522.
- [24] Yixin Liu, Shiyuan Li, Yu Zheng, Qingfeng Chen, Chengqi Zhang, and Shirui Pan. 2024. Arc: A generalist graph anomaly detector with in-context learning. *Advances in Neural Information Processing Systems* 37 (2024), 50772–50804.
- [25] Yixin Liu, Zhao Li, Shirui Pan, Chen Gong, Chuan Zhou, and George Karypis. 2021. Anomaly detection on attributed networks via contrastive self-supervised learning. *IEEE transactions on neural networks and learning systems* 33, 6 (2021), 2378–2392.
- [26] Yixin Liu, Guilbin Zhang, Kun Wang, Shiyuan Li, and Shirui Pan. 2025. Graph-Augmented Large Language Model Agents: Current Progress and Future Prospects. *arXiv preprint arXiv:2507.21407* (2025).
- [27] Xiaoxiao Ma, Jia Wu, Shan Xue, Jian Yang, Chuan Zhou, Quan Z Sheng, Hui Xiong, and Leman Akoglu. 2021. A comprehensive survey on graph anomaly detection with deep learning. *IEEE Transactions on Knowledge and Data Engineering* 35, 12 (2021), 12012–12038.
- [28] Julian John McAuley and Jure Leskovec. 2013. From amateurs to connoisseurs: modeling the evolution of user expertise through online reviews. In *Proceedings of the 22nd international conference on World Wide Web*. 897–908.
- [29] Rui Miao, Yixin Liu, Yili Wang, Xu Shen, Yue Tan, Yiwei Dai, Shirui Pan, and Xin Wang. 2025. BlindGuard: Safeguarding LLM-based Multi-Agent Systems under Unknown Attacks. *arXiv preprint arXiv:2508.08127* (2025).
- [30] Junjun Pan, Yixin Liu, Xin Zheng, Yizhen Zheng, Alan Wee-Chung Liew, Fuyi Li, and Shirui Pan. 2025. A label-free heterophily-guided approach for unsupervised graph fraud detection. In *Proceedings of the AAAI Conference on Artificial Intelligence*, Vol. 39. 12443–12451.
- [31] Junjun Pan, Yixin Liu, Yizhen Zheng, and Shirui Pan. 2023. PREM: A Simple Yet Effective Approach for Node-Level Graph Anomaly Detection. In *2023 IEEE International Conference on Data Mining (ICDM)*. IEEE, 1253–1258.
- [32] Zhen Peng, Minnan Luo, Jundong Li, Huan Liu, Qinghua Zheng, et al. 2018. ANOMALOUS: A Joint Modeling Approach for Anomaly Detection on Attributed Networks. In *IJCAI*, Vol. 18. 3513–3519.
- [33] Bryan Perozzi and Leman Akoglu. 2016. Scalable anomaly ranking of attributed neighborhoods. In *Proceedings of the 2016 SIAM International Conference on Data Mining*. SIAM, 207–215.
- [34] Oleg Platonov, Denis Kuznedelev, Michael Diskin, Artem Babenko, and Liudmila Prokhorenkova. 2023. A critical look at the evaluation of GNNs under heterophily: Are we really making progress? *arXiv preprint arXiv:2302.11640* (2023).
- [35] Tahereh Pourhabibi, Kok-Leong Ong, Booi H Kam, and Yee Ling Boo. 2020. Fraud detection: A systematic literature review of graph-based anomaly detection approaches. *Decision Support Systems* 133 (2020), 113303.
- [36] Hezhe Qiao and Guansong Pang. 2023. Truncated affinity maximization: One-class homophily modeling for graph anomaly detection. *Advances in Neural Information Processing Systems* 36 (2023), 49490–49512.
- [37] Hezhe Qiao, Hanghang Tong, Bo An, Irwin King, Charu Aggarwal, and Guansong Pang. 2024. Deep graph anomaly detection: A survey and new perspectives. *arXiv preprint arXiv:2409.09957* (2024).
- [38] Shebuti Rayana and Leman Akoglu. 2015. Collective opinion spam detection: Bridging review networks and metadata. In *Proceedings of the 21th acm sigkdd international conference on knowledge discovery and data mining*. 985–994.
- [39] Prithviraj Sen, Galileo Namata, Mustafa Bilgic, Lise Getoor, Brian Gallagher, and Tina Eliassi-Rad. 2008. Collective classification in network data. *AI magazine* 29, 3 (2008), 93–93.
- [40] Xu Shen, Yixin Liu, Yiwei Dai, Yili Wang, Rui Miao, Yue Tan, Shirui Pan, and Xin Wang. 2025. Understanding the Information Propagation Effects of Communication Topologies in LLM-based Multi-Agent Systems. *arXiv preprint arXiv:2505.23352* (2025).
- [41] Indro Spinelli, Simone Scardapane, and Aurelio Uncini. 2020. Adaptive propagation graph convolutional network. *IEEE Transactions on Neural Networks and Learning Systems* 32, 10 (2020), 4755–4760.
- [42] Ke Sun, Zhouchen Lin, and Zhanxing Zhu. 2020. Multi-stage self-supervised learning for graph convolutional networks on graphs with few labeled nodes. In *Proceedings of the AAAI conference on artificial intelligence*, Vol. 34. 5892–5899.
- [43] Jianheng Tang, Fengrui Hua, Ziqi Gao, Peilin Zhao, and Jia Li. 2023. Gadbench: Revisiting and benchmarking supervised graph anomaly detection. *Advances in Neural Information Processing Systems* 36 (2023), 29628–29653.
- [44] Jianheng Tang, Jiajin Li, Ziqi Gao, and Jia Li. 2022. Rethinking graph neural networks for anomaly detection. In *International Conference on Machine Learning*. PMLR, 21076–21089.

- [45] Lei Tang and Huan Liu. 2009. Relational learning via latent social dimensions. In *Proceedings of the 15th ACM SIGKDD international conference on Knowledge discovery and data mining*. 817–826.
- [46] Petar Veličković, Guillem Cucurull, Arantxa Casanova, Adriana Romero, Pietro Lio, and Yoshua Bengio. 2017. Graph attention networks. *arXiv preprint arXiv:1710.10903* (2017).
- [47] Mark Weber, Giacomo Domeniconi, Jie Chen, Daniel Karl I Weidele, Claudio Bellei, Tom Robinson, and Charles E Leiserson. 2019. Anti-money laundering in bitcoin: Experimenting with graph convolutional networks for financial forensics. *arXiv preprint arXiv:1908.02591* (2019).
- [48] Felix Wu, Amauri Souza, Tianyi Zhang, Christopher Fifty, Tao Yu, and Kilian Weinberger. 2019. Simplifying graph convolutional networks. In *International conference on machine learning*. PMLR, 6861–6871.
- [49] Zonghan Wu, Shirui Pan, Fengwen Chen, Guodong Long, Chengqi Zhang, and S Yu Philip. 2020. A comprehensive survey on graph neural networks. *IEEE transactions on neural networks and learning systems* 32, 1 (2020), 4–24.
- [50] Zhiming Xu, Xiao Huang, Yue Zhao, Yushun Dong, and Jundong Li. 2022. Contrastive attributed network anomaly detection with data augmentation. In *Pacific-Asia conference on knowledge discovery and data mining*. Springer, 444–457.
- [51] Xiaoyu Yang, Yuefei Lyu, Tian Tian, Yifei Liu, Yudong Liu, and Xi Zhang. 2021. Rumor detection on social media with graph structured adversarial learning. In *Proceedings of the twenty-ninth international conference on international joint conferences on artificial intelligence*. 1417–1423.
- [52] Wentao Zhang, Zeang Sheng, Ziqi Yin, Yuezihan Jiang, Yikuan Xia, Jun Gao, Zhi Yang, and Bin Cui. 2022. Model degradation hinders deep graph neural networks. In *Proceedings of the 28th ACM SIGKDD conference on knowledge discovery and data mining*. 2493–2503.
- [53] Yu Zheng, Ming Jin, Yixin Liu, Lianhua Chi, Khoa T Phan, and Yi-Ping Phoebe Chen. 2021. Generative and contrastive self-supervised learning for graph anomaly detection. *IEEE Transactions on Knowledge and Data Engineering* 35, 12 (2021), 12220–12233.